

PAPER

[View Article Online](#)
[View Journal](#) | [View Issue](#)Cite this: *Dalton Trans.*, 2022, **51**,
6756Organoaluminum hydrides catalyzed
hydroboration of carbonates, esters, carboxylic
acids, and carbon dioxide†Ben Yan,^{‡a} Sayan Dutta,^{‡b} Xiaoli Ma,^{ID} *^a Congjian Ni,^a Debasis Koley,^{ID} *^b
Zhi Yang^{*a} and Herbert W. Roesky^{ID} *^c

The reductive functionalization of the C=O unit of carbonates, carboxylic acids, esters, and CO₂, respectively has received great attention since its introduction. This method is often used industrially for the synthesis of high value-added energy products in chemistry. This opens up a new way forward to reduce greenhouse gases and the consumption of traditional energy sources. Herein, we report an earth-abundant, cheap, and readily available aluminum dihydride, which can catalyze the reduction of a range of carbonates, esters, carboxylic acids, and CO₂, respectively in the presence of pinacolborane as a reducing agent. Moreover, we demonstrate that the reaction can proceed to obtain good yield products under mild conditions, with low catalyst loading and solvent-free reactions. The mechanism of the catalytic reduction of carbonates has been investigated.

Received 12th March 2022

Accepted 8th April 2022

DOI: 10.1039/d2dt00785a

rsc.li/dalton

Introduction

The reduction reaction plays a pivotal role in chemical transformation, synthesis, and recycling. Therefore, reduction reactions, especially hydrogenation reactions, have been widely used in traditional industrial, agricultural, and energy fields during the last decades. Hydroboration reaction has become a hot research topic due to its low toxicity, high reactivity, and high selectivity control in recent years as an alternative method to the traditional hydrogenation reduction process. However, it is significant to have a selective and efficient method to reduce the conversion of CO₂ and derivatives into a wide range of C1 chemicals such as formaldehyde, methanol, etc.¹ Therefore, the hydroboration of carbonates, carboxylic acids, esters, and carbon dioxide itself, containing C=O units are great precursors.

The research on the synthesis and properties of compounds with low-valent elements and low coordination numbers of main group species are gradually developed over the past few years.^{2–6} In comparison with transition metals, most of the

main group metals have the characteristics of earth-abundant, cheap, and environmentally friendly elements. Among them, organoaluminum compounds are attracting much attention due to the strong Lewis acidity of the central aluminum atom, which can be used for reactions with electron-rich compounds. This advantage has attracted chemists to struggle along with the development of new aluminum compounds for catalysts.^{7,8} In 2015 our group presented a method for the selective hydroboration of aldehydes and ketones using an organoaluminum hydride as an excellent catalyst.⁹ Afterward we expanded the substrates to alkynes,¹⁰ nitriles,¹¹ and carbodiimides,^{12,13} while aluminum compounds for catalysis also made great progress.^{14–21} Given the growing interest in aluminum-catalyzed organic reactions and the fixation of carbon dioxide and its derivatives, we aimed our target at Al-catalyzed reductions. Surprisingly, we discovered that the hydroboration reactions of a broad range of cyclic and linear organic carbonates, esters, carboxylic acids, and even CO₂ are efficiently catalyzed by aluminum hydrides. The reactions proceed under mild conditions. Herein, we report our results (Scheme 1).

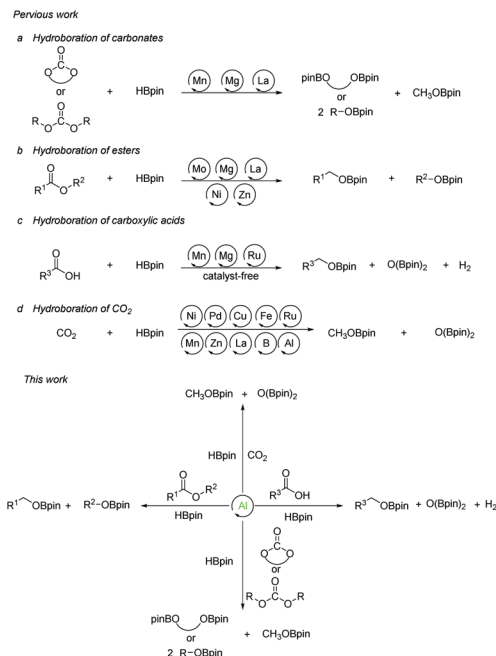
Results and discussion

Reduction of carbonates

There is a common method employed in industry to reduce greenhouse gas emissions by reacting carbon dioxide with epoxides to form organic carbonates. Carbonates are widely used as solvents in various chemical reactions due to their

^aSchool of Chemistry and Chemical Engineering, Beijing Institute of Technology, Beijing, P. R. China. E-mail: maxiaoli@bit.edu.cn, zhiyang@bit.edu.cn^bDepartment of Chemical Sciences, Indian Institute of Science Education and Research (IISER) Kolkata, Mohanpur 741 246, India. E-mail: koley@iiserkol.ac.in^cDr. P. H. W. Roesky, Institut für Anorganische Chemie, Georg-August-Universität Göttingen, Tammannstr. 4, 37077 Göttingen, Germany. E-mail: hroesky@gwdg.de† Electronic supplementary information (ESI) available. See DOI: <https://doi.org/10.1039/d2dt00785a>

‡ These authors contributed equally to this work.



Scheme 1 Previous approaches towards the hydroboration reactions of organic commodities and the progress of our strategy.

excellent stability.²² Therefore, the reduction of carbonates becomes quite difficult. Carbonates are often directly catalyzed by hydrogenation enabling the conversion of CO₂ into value-added chemicals such as methanol or diols. However, these reactions require either high temperature and pressure or transition metals as catalysts.^{23–30} Hence, the hydroboration reaction of carbonates can be used as an alternative method to avoid the use of flammable and explosive gases or transition metals as reductants. Nevertheless, there are a few reports on the hydroboration of carbonates (Scheme 1).^{29,31–34} Thus, it is crucial to develop hydroboration reactions of Al-catalyzed carbonates under mild conditions.

We selected two reported aluminum hydrides LAlH₂ (L = HC(CMeNAr)₂ Ar = 2,6 - iPr₂C₆H₃) (**1**, Fig. 1) and L'AlH₂ (L' = HC(CMeNAr)₂, Ar = 2,6 - Et₂C₆H₃) (**2**, Fig. 1) as catalysts and started our initial investigation by utilizing cyclic carbonate **3a** as substrate and pinacolborane (HBpin) as reductant under the neat condition with catalyst loading of 5 mol%. In the first test, two aluminum hydrides were used as catalysts in the reactions which were not completed at 50 °C after 8 h (Table 1,

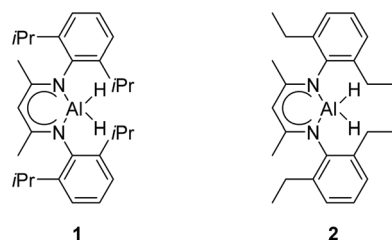


Fig. 1 The structures of two aluminum hydrides.

Table 1 Optimization of Al-catalyzed hydroboration of carbonates^a

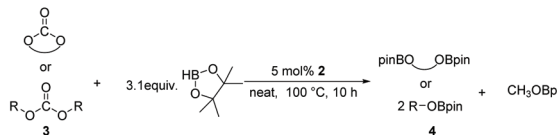
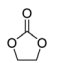
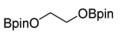
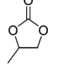
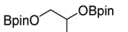
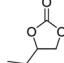
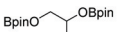
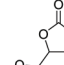
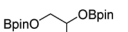
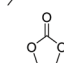
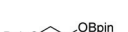
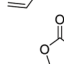

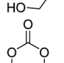

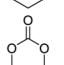

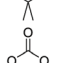

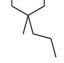
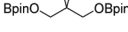
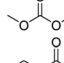
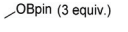
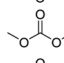

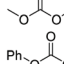
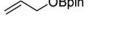
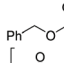

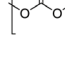


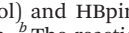
Entry	Cat.	T (°C)	t (h)	Yield ^b (%)
1	1	50	8	46
2	2	50	8	59
3	1	50	10	67
4	2	50	10	78
5	2	80	10	84
6	2	100	10	99
7 ^c	2	100	10	96
8 ^d	2	100	10	94
9 ^e	2	100	10	91
10	—	100	10	0

^a Ethylene carbonate (**3a**) (1 mmol), HBpin (3.1 equiv.), catalysts (5 mol%). ^b The reaction was monitored by ¹H NMR spectroscopy. ^c Toluene as a solvent. ^d THF as a solvent. ^e The loading of the catalyst was 3 mol%.

entries 1 and 2). Extending the time to 10 h showed that large amounts of carbonate were still observed in the crude product even though the yield was improved (Table 1, entries 3 and 4). Based on the results, we noticed that aluminum dihydride **2** showed superior catalytic performance when compared with **1**. The temperature of the reaction system was increased to 80 °C as a further step to achieve higher yields (Table 1, entry 5). To our delight, carbonate **3a** was completely transformed at 100 °C after 10 h (Table 1, entry 6). Furthermore, when toluene and THF were selected as solvents, the yields even slightly decreased (Table 1, entries 7 and 8). With a lower loading of catalyst **2** to 3 mol%, only 91% yield was obtained (Table 1, entry 9). No expected product was formed when no catalyst was added in the control experiment (Table 1, entry 10).

Following the optimal conditions, we investigated the substrate scope and limitation of the hydroboration of different cyclic and linear carbonates (Table 2). All reactions gave good yields using 5 mol% loadings of catalyst **2** at 100 °C under solvent-free conditions within 10 h. Five-membered ring carbonates bearing aliphatic groups such as Me and Et showed quantitative yield under the same condition of ethylene carbonate (Table 2, entries 2 and 3). When the branched-chain was replaced by the methoxy group the conversion of the hydroboration product is slightly reduced (Table 2, entry 4). Interestingly, we observed that the reduction of unsaturated carbonate occurred at the carbonate functional part rather than at the olefin group (Table 2, entry 5). 4-(Hyoxymethyl)-1,3-dioxolan-2-one bearing a hydroxyl group reacted with 4.1 equivalent of HBpin and resulted in a nearly quantitative yield of the corresponding boronate ester (Table 2, entry 6). Organic carbonates containing a six-membered ring were able to produce effective yields by reduction (Table 2, entries 7 and 9). However, 5,5-dimethyl-1,3-dioxane-2-one was observed only in 60% yield and this phenomenon may be related to the low solubility of the substrate in HBpin (Table 2, entry 8). The

Table 2 Hydroboration of carbonates catalyzed by **2**^a

				
Entry	Carbonate	Product		Yield ^b (%)
1	 3a	 4a		99
2	 3b	 4b		99
3	 3c	 4c		99
4	 3d	 4d		94
5	 3e	 4e		99
6 ^c	 3f	 4f		99
7	 3g	 4g		99
8	 3h	 4h		60
9	 3i	 4i		99
10	 3j	 4j		99
11	 3k	 4k		99
12	 3l	 4l		99
13	 3m	 4m		93
14	 3n	 4n		86
15	 3o	 4o		89
16 ^d	 3p	 4b		97

^a Reaction conditions: **3** (1 mmol) and HBpin (3.1 mmol, 3.1 equiv.) and **2** (5 mol%), 100 °C for 10 h. ^b The reaction was monitored by ¹H NMR spectroscopy. ^c 4.1 equiv. of HBpin was used. ^d Average *M_n* of starting material: ~50 000.

result is consistent with that reported in the article by Leitner *et al.* in 2018.²⁹

Typically, linear carbonates are more challenging to reduce than cyclic carbonates. Gratifyingly, dimethyl, diethyl, and ethyl methyl carbonates could achieve full conversion with excellent yields (Table 2, entries 10–12). The hydroboration of allyl methyl carbonate which contains the olefin group also accomplished 93% yield (Table 2, entry 13). Subsequently, we shifted our interest to the reduction of dibenzyl carbonate and

diphenyl carbonate which underwent slightly decreased yields compared to the linear carbonates (Table 2, entries 14 and 15). To further investigate the applicability of aluminum hydride compound for catalyzing carbonates, we selected polypropylene carbonate as the reaction substrate which can be synthesized by propylene and CO₂ industrially. Remarkably, the yield of the hydroboration product can achieve 97% conversion (Table 2, entry 16). The product can be further reacted with HCl and purified by flash chromatography to obtain the corresponding alcohol. The catalysts **1** and **2** can be easily synthesized by β-diimine and LiAlH₄ or AlH₃·NMe₃ in yields greater than 90% at the gram scale. Even the Al-catalyzed protocol is not more effective than alkaline earth or transition metals systems (Al: 100 °C, 10 h, 99% yield *vs.* Mg/Mn: r.t. –90 °C, 3–8 h, 99% yield), it is also confirmed that our aluminum-based metal catalysts are based on low-cost and easily available when compared with existing protocols.^{29–32}

Reduction of esters

The ester linkages are both prevalent in cellulose and vegetable oils in nature and an essential transformation process in the synthesis of organic as well as of drug entities. Nevertheless, it is very challenging to reduce esters compared with the carbonyl groups of aldehydes and ketones on account of the thermodynamic inertness.³⁵ Typically, the transformation is achieved by applying powerful reducing agents such as BH₃ and LiAlH₄ which require stringent reaction conditions and post-treatment processes.^{36–42} Therefore, the reduction of esters with boranes such as pinacolborane (HBpin) is comparatively stable and convenient to handle, thus avoiding unnecessary safety problems. As far as we know, only a few examples of hydroboration reactions of esters have been discussed in recent years and these catalysts are mainly made of rare earth and alkaline earth metals (Scheme 1).^{33,43–47} In some of the above descriptions, the ester is only served as a single example of substrates that have been published.^{43,45,48} Thus, it is necessary to develop a general protocol for the aluminum system to catalyze the hydroboration of esters.

Initially, we explored whether the ester and pinacolborane would react spontaneously for lack of catalyst, unfortunately, no exciting results were detected even at temperatures up to 60 °C (see the ESI Table S1,† entries 1 and 2). Further, a detailed investigation by using aluminum dihydride **2** as a catalyst was investigated for the reduction of esters (Table S1,† entries 3–7). Noticeably, the yield increased with the rising temperature and the prolonged reaction time. Ultimately, the reaction yield achieved 99% within 12 h at a catalyst loading of 5 mol% with a temperature of 60 °C.

Inspired by the screening data, we evaluated the applicability of aluminum compound **2** to catalyze the hydroboration of varieties of ester substrates under optimized conditions. Table 3 shows the full scope of investigated esters. In the case of esters featuring different substituents, quantitative conversion was performed in 12 hours using 5 mol% of compound **2** at 60 °C no matter of the aliphatic or aromatic groups (Table 3, entries 1–7). It should be pointed out particularly that this



Table 3 Hydroboration of esters catalyzed by **2**^a

$\text{R}^1-\text{C}(=\text{O})-\text{O}-\text{R}^2 + 2.1 \text{ HBpin} \xrightarrow[60^\circ\text{C}, 12 \text{ h}]{5 \text{ mol\% } \mathbf{2}} \text{R}^1-\text{CH}_2-\text{OBpin} + \text{R}^2-\text{OBpin}$					
Entry	Ester	Product	Yield ^b (%)		
1			99	5a	6a
2 ^c			99	5b	6b
3			99	5c	6c
4 ^d			99	5d	6d
5 ^c			99	5e	6e
6 ^c			99	5f	6f
7			99	5g	6g
8			99	5h	6h
9 ^e			99	5i	6i
10			99	5j	6j
11 ^c			98	5k	6k
12 ^d			99	5l	6l
13 ^d			99	5m	6m
14 ^d			98	5n	6n
15 ^d			99	5o	6o

^a Reaction conditions: **5** (1 mmol), HBpin (2.1 mmol, 2.1 equiv.) and **2** (5 mol%), 60 °C for 12 h. ^b The reaction was monitored by ¹H NMR spectroscopy. ^c Product + EtOBpin. ^d Product + MeOBpin. ^e 4.2 equiv. of HBpin was used.

catalytic system is more selective for ester groups than olefin groups (Table 3, entry 4). Next, we extended our substrate scope to cyclic esters including lactide which transformed the corresponding dialkoxy boronic esters in excellent yield (Table 3, entries 8–10). To obtain the information on the catalytic reaction of heterocyclic ester, we combined 2-coumaranone with HBpin to reach quantitative yield (Table 3, entry 11). Apart from the above substrates, a further range of electron-donating and electron-withdrawing group substrates proved to be suitable for this transition. In summary, we confirmed that this catalyst has good functional group tolerance (Table 3, entries 12–15). Similarly, esters can get the consistent conclusion with carbonates that the Al-based catalysts are not more efficient than alkaline earth metal systems (Al: 60 °C, 12 h, 99% yield vs. Mg r.t., 0.5–1 h, 99% yield).^{32,46}

Reduction of carboxylic acids

As the broad basic unit in organic chemistry, alcohols have a wide range of applications in the fine chemical, agricultural, and pharmaceutical industries.^{49–52} It is important not only to generate novel functional groups in organic synthesis but also to enable biomass feedstocks for utilizing high-value chemicals. The conventional approach is to utilize metal hydrides such as LiAlH₄ or Zn(BH₄)₂ as reducing agents, but the safety of the reaction and the subsequent disposal of the reactants pose problems.^{53,54} Moreover, hydrogen gas is considered to be one of the most efficient reagents for reduction. However, the extremely flammable nature of hydrogen and the demanding requirements for equipment to withstand high pressure and temperature conditions restrict its widespread application.^{30,55,56} Another methodology for the reduction of carboxylic acids to alcohols is through hydrosilylation, which suffers from the disadvantages of requiring transition metals (Ru, Rh, Ir, Fe, Mn, Cu, *etc.*) as catalysts that limit the range of substrates or require a light-mediated process.^{57–64}

Gunanathan and co-workers described the first example of a ruthenium-based catalyst acting on the reaction of the carboxylic acid with HBpin. The resulting alkyl boronate was treated hydrolytically to produce the primary alcohol. This procedure opened the way for the study of hydroboration of carboxylic acids.⁶⁵ Previously, Leitner *et al.*, as well as Maji *et al.*, reported manganese-catalyzed borohydride reactions of carboxylic acids.^{29,66} However, to our knowledge, there is only one case of main group metal-catalyzed hydroboration reaction reported of carboxylic acids.⁶⁷ With the increasing demand for transition metal substitution and green catalysts, there is a strong need to extend aluminum-catalyzed hydroboration reactions with unsaturated substrates to carboxylic acids, considering the interest in developing new catalysts for carboxylic acid reduction. During this protocol, there are several research groups, which have recently reported such reactions under catalyst-free and solvent-free conditions. Nevertheless, conditions such as excessive HBpin or heating are required to achieve a successful synthesis (Scheme 1).^{68–70}

The reaction condition of the standard scheme which was obtained by screening the conditions using benzoic acid as the reaction substrate (see the ESI Table S2†). Firstly, the hydroboration reaction of benzoic acid with 3.1 equiv. of HBpin was carried out at room temperature under neat conditions. Only 57% yield was obtained after 1 hour (Table S2,† entry 1). Then, the HBpin was increased to 3.3 equiv. which resulted in a yield of 63% under the same condition (Table S2,† entry 2). We were gratified to find that the yield excellently increased after the reaction time was extended to 2 h (Table S2,† entries 3 and 4). In addition, a parallel experiment was conducted by decreasing compound **2** to 1 mol%, and the production was subsequently reduced (Table S2,† entry 5). When no catalyst was employed in the reaction, a sharp decline in the corresponding benzyl borate was detected (Table S2,† entries 6 and 7). Notably, the main group Al-catalyzed protocol is more effective when compared with transition metal systems (Al: r.t., 2 h,



99% yield vs. Ru/Mn: 60–115 °C, 20–24 h, 99% yield).^{29,65} Certainly, Al-catalyst has significant advantages over catalyst-free systems and lower reaction temperatures.

Taking the optimized reaction into account, we exploited the scope and limitations of the hydroboration of carboxylic acid. As shown in Table 4, we realized that either the aromatic acids with an electron-donating group (–Me, –*t*Bu, –OMe) or electron-withdrawing substituents (–F, –Cl, –NO₂, –CN), could afford quantitative yields of the corresponding boronate ester in 2 hours (Table 4, entries 2–8). Compounds with larger steric hindrances like diphenylacetic acid and 2-naphthoic acid also

underwent a reduction reaction in excellent yield (Table 4, entries 9 and 10). Remarkably, 2-thiophenecarboxylic acid proceeded to hydroboration with HBpin, and a 99% yield was observed (Table 4, entry 11). Then, we expanded the substrate scope to the aliphatic carboxylic acids. Surprisingly, we observed that aliphatic carboxylic acids were obtained in quantitative yields under the same conditions which supported the suitability of the Al-catalyst for structurally diverse carboxylic acid substrates (Table 4, entries 12–18).

Reduction of carbon dioxide

The high-performance hydroboration catalysis of various substrates containing C=O functional groups by aluminum compounds prompted us to explore directly the reduction of CO₂. As a sustainable C1 feedstock, there is interest in converting from CO₂ to products such as formaldehyde and methanol, which are currently synthesized from non-renewable feedstocks.^{71–80} Lately, the hydroboration of CO₂ has received significant attention in organic synthesis. The majority of the reported catalytic systems focus on transition-metal complexes (including Ni,^{81,82} Pd,^{83–85} Cu,⁸⁶ Fe,⁸⁷ Ru,^{88,89} Co,⁹⁰ Mn,²⁹ and Zn⁹¹), alkali metal complexes,^{45,92} and other main-group catalysts.^{93–98} However, hydroboration of CO₂ by using an aluminum catalyst is still rare (Scheme 1).^{99,100}

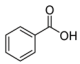
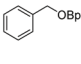
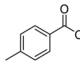
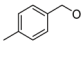
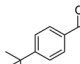
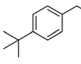
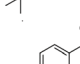
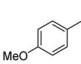
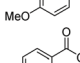
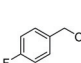
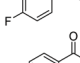
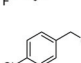
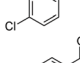
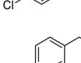
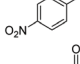
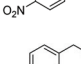
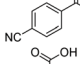
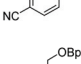
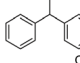
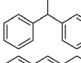
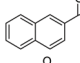
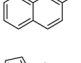
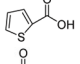
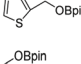
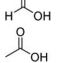
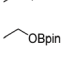
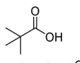
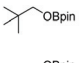
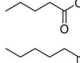
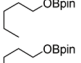
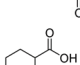
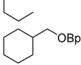
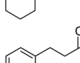
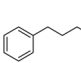
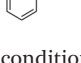

In this case, we increased the reaction temperature and catalyst ratio to 10 mol% to ensure adequate consumption of HBpin. The experimental results showed that CO₂ could be fully reduced with a yield of 95% after 48 h of stirring. With this exciting result, it offers a new approach for the direct reduction conversion of CO₂ (Scheme 2).

It is interesting that the hydroboration of CO₂ with HBpin using the similar organoaluminum hydrides catalyst was not observed in the previous report from Aldridge and co-workers.¹⁰¹ However, organoaluminum hydrides can catalyze CO₂ this was observed by So and his colleagues, and they explained the reaction mechanism using DFT calculations.⁹⁹ This phenomenon deserves to be further explored in our future work.

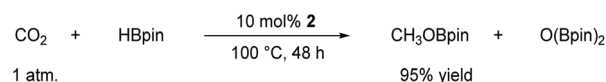
Proposed mechanism

To further understand the mechanism, we chose catalytic carbonate as the template and conducted several additional control experiments. An equimolar mixture of organoaluminum catalyst 2 with ethylene carbonate 3a and HBpin, respectively, was reacted at room temperature, and the results were analyzed by ¹H NMR spectroscopy. We found that only the reaction of 2 with ethylene carbonate showed a new single resonance at 4.32 ppm in the ¹H NMR with a 2H intensity by integration which is presumable to form an aluminum–oxygen

Table 4 Hydroboration of carboxylic acid catalyzed by 2^a

$\text{R}^3\text{COOH} + 3.3 \text{ HBpin} \xrightarrow[\text{neat, n.t., 2 h}]{2 \text{ mol\% } 2} \text{R}^3\text{CH}_2\text{OBpin} + \text{O}(\text{Bpin})_2 + \text{H}_2$				
Entry	Carboxylic acid	Product		Yield ^b (%)
1	 7a	 8a		99
2	 7b	 8b		99
3	 7c	 8c		99
4	 7d	 8d		96
5	 7e	 8e		98
6	 7f	 8f		99
7	 7g	 8g		97
8	 7h	 8h		99
9	 7i	 8i		98
10	 7j	 8j		92
11	 7k	 8k		99
12	 7l	 8l		99
13	 7m	 8m		99
14	 7n	 8n		99
15	 7o	 8o		97
16	 7p	 8p		99
17	 7q	 8q		99
18	 7r	 8r		99

^a Reaction conditions: 7 (1 mmol), HBpin (3.3 mmol, 3.3 equiv.) and 2 (2 mol%), room temperature for 12 h. ^b The reaction was monitored by ¹H NMR spectroscopy with mesitylene as an internal standard.



Scheme 2 Aluminum-catalyzed hydroboration of CO₂.



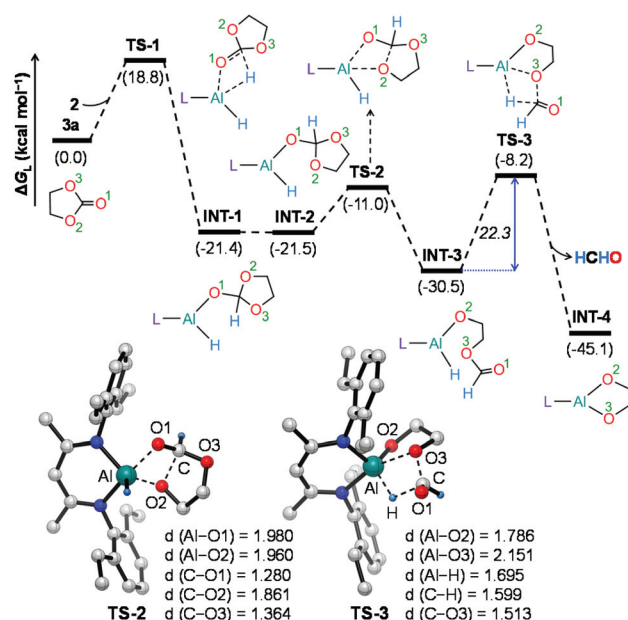


Fig. 2 Energy profile for the formation of the intermediate **INT-4** and formaldehyde. Optimized geometries of the transition states **TS-2** and **TS-3** with important geometrical parameters are also provided. Bond distances (d) are in angstroms (Å). Only key hydrogen atoms are shown for clarity. $\text{L} = \text{HC}(\text{CMeNAr})_2$, $\text{Ar} = 2,6 - \text{Et}_2\text{C}_6\text{H}_3$.

compound (see ESI† for details). A detailed theoretical exploration of aluminum-catalyzed hydroboration of carbonates would be of great importance and necessary to unravel the complete mechanistic picture for this kind of fascinating system. Therefore, quantum chemical calculations were performed at the R-BP86-D3/def2-TZVP//R-BP86/def2-SVP level¹⁰² to explore the mechanistic avenues in aluminum dihydride 2-

catalyzed hydroboration of cyclic carbonate **3a**, leading to the formation of **4a** and methoxyboronic acid pinacol ester (**CH₃OBpin**). The reaction initiates with insertion of the carbonyl group of **3a** into the Al-H bond in the catalyst to afford a significantly stable intermediate **INT-1** (Fig. 2). This step needs to surmount an energy barrier of 18.8 kcal mol⁻¹. **INT-1** then rearranges to **INT-2** to facilitate the approach of the oxygen (O2) center towards aluminum, which leads to the formation of an appreciably stable intermediate **INT-3** via **TS-2**. The intra-molecular hydride transfer from the aluminum center to the carbonyl carbon of **INT-3** in the subsequent step promotes the liberation of formaldehyde (**HCHO**), giving rise to the generation of a remarkably stable intermediate **INT-4**. The incoming pinacolborane (**HBpin**) gets coordinated to the oxygen center (O3) in the resulting intermediate **INT-4** to furnish a slightly less stable adduct **INT-5** via **TS-4** (Fig. 3).¹⁰³ The subsequent hydride transfer from boron to aluminum with simultaneous Al-O3 bond rupture leads to the generation of **INT-6**. The step requires an intrinsic energy barrier of 5.9 kcal mol⁻¹ and the single imaginary mode in the corresponding transition state **TS-5** animates the breaking of Al-O3 (2.254 Å) and B-H (1.741 Å) bonds with concomitant Al-H (1.659 Å) bond formation. **INT-6** then rearranges to **INT-7** and the coordination of the second **HBpin** to the oxygen center (O2) in **INT-7** results in **INT-8** via **TS-6**. This step needs to overcome an energy barrier of 9.0 kcal mol⁻¹, indicating a slightly higher energy barrier required for the coordination of the second pinacolborane compared to the first one. **INT-8** then undergoes similar hydride transfer to afford the desired product **4a** with the regeneration of the catalyst. This step corresponding to an overall activation barrier of 25.1 kcal mol⁻¹ is the rate-determining step for the catalytic transformation. The calculated rate-limiting energy barrier is reasonable under the solvent-free, 100 °C reaction conditions.

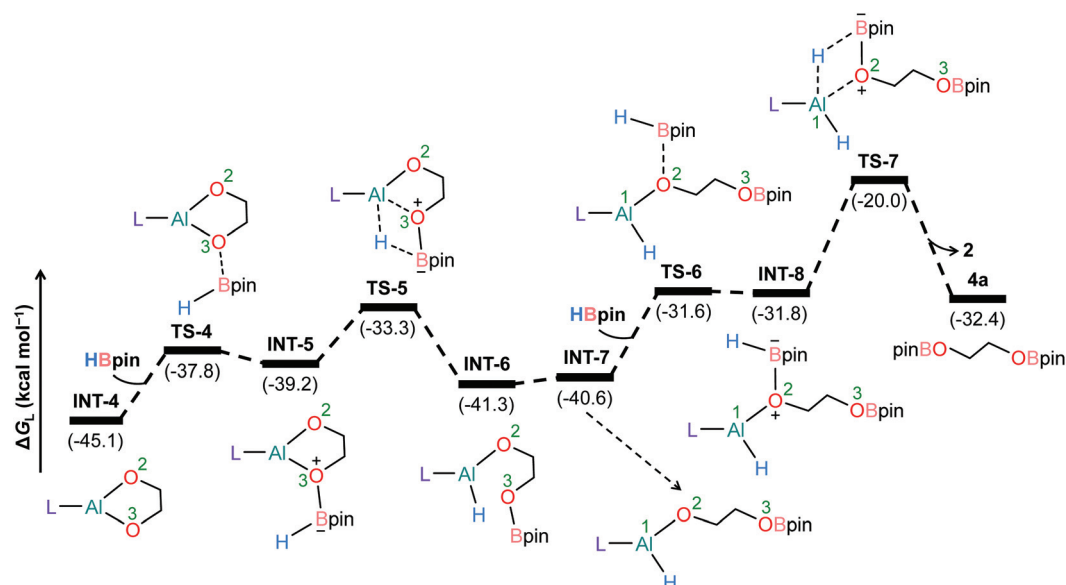


Fig. 3 Energy profile for the 2-catalyzed formation of **4a**. $\text{L} = \text{HC}(\text{CMeNAr})_2$, $\text{Ar} = 2,6 - \text{Et}_2\text{C}_6\text{H}_3$.

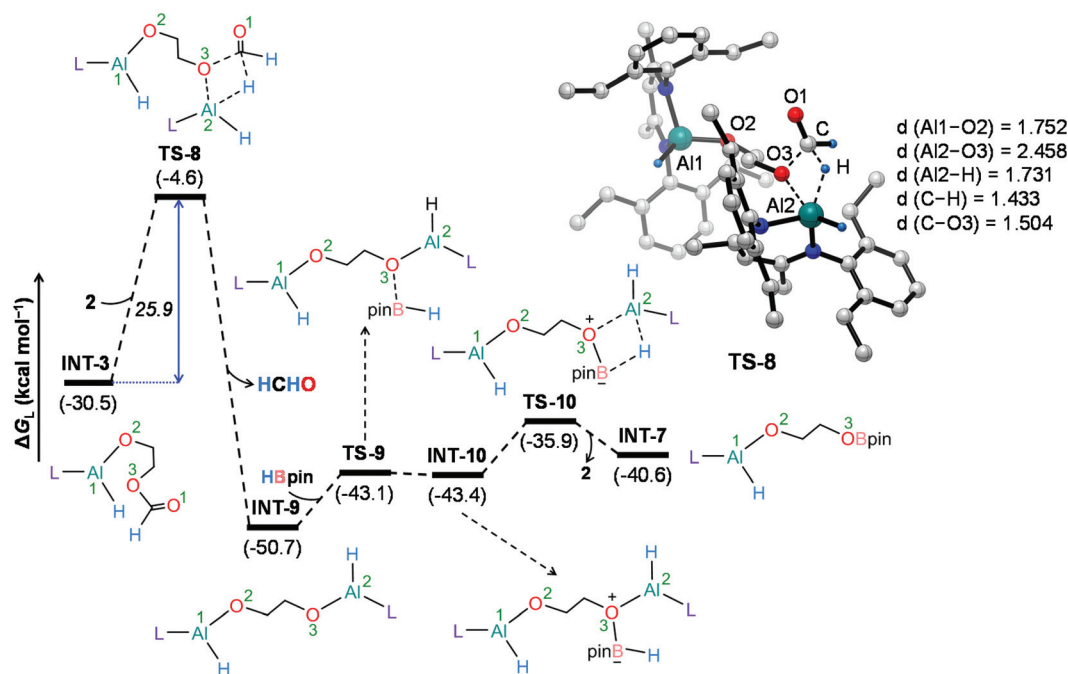


Fig. 4 Energy profile for the alternative pathway leading to the formation of the intermediate INT-7. Optimized geometry of the transition state TS-8 with important geometrical parameters is also provided. Bond distances (d) are in angstroms (Å). Only key hydrogen atoms are shown for clarity. L = HC(CMeNAr)₂, Ar = 2,6 Et₂C₆H₃.

We have also explored the alternative pathway leading to the generation of the intermediate INT-7 (Fig. 4). The intermolecular hydride transfer from the catalyst to the carbonyl carbon of INT-3 furnishes a remarkably stable intermediate INT-9 with the liberation of formaldehyde. This step needs to

surmount an activation barrier of 25.9 kcal mol⁻¹. Then similar HBpin coordination followed by hydride transfer to the aluminum center with the release of catalyst molecule affords INT-7. Though this reaction channel demands a slightly higher energy barrier compared to that of the intramolecular

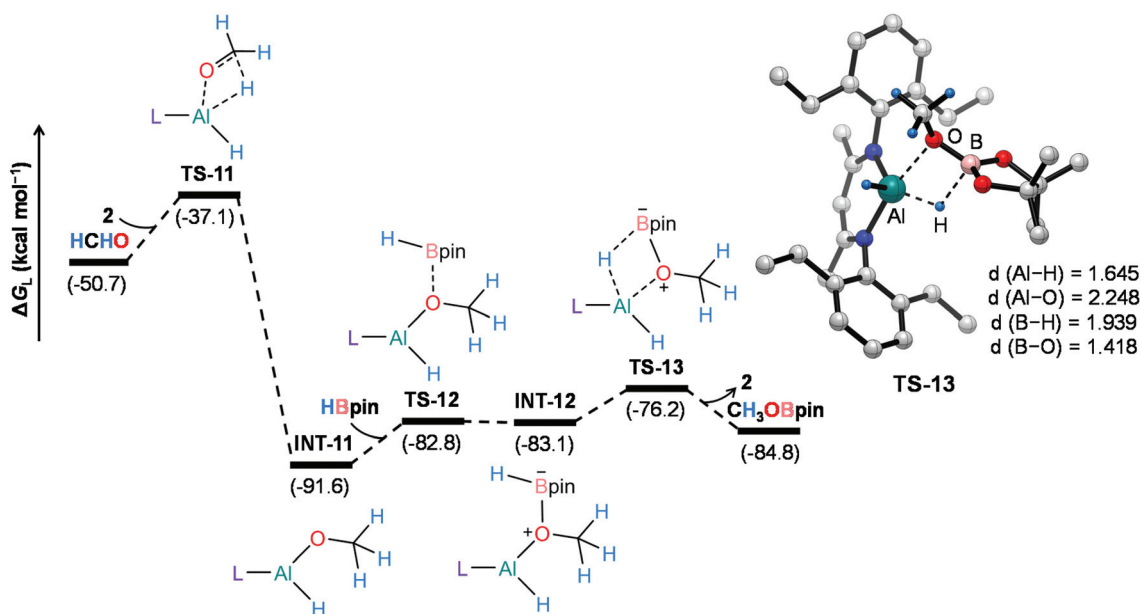


Fig. 5 Energy profile for the 2-catalyzed formation of CH₃OBpin. Optimized geometry of the transition state TS-13 with important geometrical parameters is also provided. Bond distances (d) are in angstroms (Å). Only key hydrogen atoms are shown for clarity. L = HC(CMeNAr)₂, Ar = 2,6 Et₂C₆H₃.



hydride transfer ($22.3 \text{ kcal mol}^{-1}$), participation of a second catalyst molecule in the reaction channel is less likely to operate under the experimental conditions. We have also checked another alternative route for the formation of **INT-7** involving a substantially stable cyclic intermediate **INT-13** (Fig. S5†). However, the second hydride transfer from aluminum to the carbonyl carbon in **INT-2** with concurrent C–O2 bond breaking to afford **INT-13** demands a drastically high energy barrier of $67.4 \text{ kcal mol}^{-1}$. Additionally, participation of **HBpin** instead of **2** in the generation of formaldehyde from **INT-3** also involves **TS-18** which shows a reasonably high barrier height of $36.5 \text{ kcal mol}^{-1}$ and therefore, can be safely discarded on the kinetic ground (Fig. S6†). Moreover, we have performed distortion–interaction analysis to cast light on the origin of activation barriers for **TS-8** and **TS-18** (Tables S3 and S4†).^{104–106} Though the distortion energy of the **INT-3** fragment is appreciably lower in **TS-18** than **TS-8** [$\Delta^\ddagger E_{\text{dist}}(\text{INT-3})$: $27.7/22.7 \text{ kcal mol}^{-1}$ in **TS-8/TS-18**], immensely larger distortion energy of the **HBpin** fragment in **TS-18** compared to the catalyst fragment in **TS-8** accounts for the substantially higher activation barrier in the former transition state [$\Delta^\ddagger E_{\text{dist}}(\text{HBpin})$: $8.6/27.8 \text{ kcal mol}^{-1}$ in **TS-8/TS-18**].

On the other hand, **2**-catalyzed hydroboration of formaldehyde furnishes **CH₃OBpin** product (Fig. 5). The insertion of formaldehyde into the Al–H bond in the catalyst initiates this reaction channel to yield substantially stable intermediate **INT-11**, accompanying a moderate energy barrier of $13.6 \text{ kcal mol}^{-1}$. The coordination of pinacolborane to the oxygen center in **INT-11** generates a slightly less stable intermediate **INT-12** via **TS-12**. Finally, the hydride transfer from boron to aluminum with concurrent Al–O bond rupture delivers **CH₃OBpin** and the catalyst also gets regenerated. This step demands an intrinsic energy barrier of $6.9 \text{ kcal mol}^{-1}$ and an overall energy barrier of $15.4 \text{ kcal mol}^{-1}$ with respect to **INT-11**. Hence, DFT calculations reveal that the aluminum dihydride species not only catalyzes the formation of **4a** but also plays a crucial role in generating formaldehyde in the catalytic system, which eventually furnishes **CH₃OBpin**. The theoretical calculation results also verify our conjecture about the control experiment (Scheme S1†).

Conclusions

In summary, we report the first excellent catalytic performance of reduction of a wide range of CO₂-derived cyclic five- and six-membered carbonates, linear carbonates, polycarbonates, by using the cheap and environmentally friendly organic aluminum hydrides under neat condition. The new protocol shows excellent capabilities in hydroboration of esters, carboxylic acids, and carbon dioxide as well. Its simplicity and versatility make it a useful protocol compared to most the hydroboration strategies for challenging C=O functionalities. In-depth mechanistic underpinning of aluminum dihydride **2**-catalyzed hydroboration of carbonate **3a** suggests a very unique reaction route with involvement of **2** in two parallel pathways, one

giving rise to product **4a** and the other to **CH₃OBpin** via hydroboration of formaldehyde generated in the catalytic system. All transformations are carried out smoothly, under neat conditions with suitable catalyst loading, and showing they're sustainable applications.

Conflicts of interest

There are no conflicts to declare.

Acknowledgements

We gratefully acknowledge financial support from the National Natural Science Foundation of China (21872005, 21671018). H. W. R. thanks the Deutsche Forschungsgemeinschaft for financial support RO224/70-1. S. D. acknowledges the CSIR, India for the Senior Research Fellowship (SRF) and IISER Kolkata for the computational facility. D. K. acknowledges the generous funding from MoE-STARS (MoE-STARS/STARS-1/255) scheme. We are thankful to the reviewers for their valuable suggestions to improve the quality of the manuscript. Dedicated to Professor Ionel Haiduc on the occasion of his 85th birthday.

Notes and references

- 1 C. Maeda, Y. Miyazaki and T. Ema, *Catal. Sci. Technol.*, 2014, **4**, 1482–1497.
- 2 P. P. Power, *Nature*, 2010, **463**, 171–177.
- 3 D. Martin, M. Soleilhavoup and G. Bertrand, *Chem. Sci.*, 2011, **2**, 389–399.
- 4 A. Schulz and A. Villinger, *Angew. Chem., Int. Ed.*, 2012, **51**, 4526–4528.
- 5 D. W. Stephan and G. Erker, *Angew. Chem., Int. Ed.*, 2010, **49**, 46–76.
- 6 C. Weetman and S. Inoue, *ChemCatChem*, 2018, **10**, 4213–4228.
- 7 P. Bag, C. Weetman and S. Inoue, *Angew. Chem., Int. Ed.*, 2018, **57**, 14394–14413.
- 8 S. Dagorne and R. Wehmschulte, *ChemCatChem*, 2018, **10**, 2509–2520.
- 9 Z. Yang, M. Zhong, X. Ma, S. De, C. Anusha, P. Parameswaran and H. W. Roesky, *Angew. Chem., Int. Ed.*, 2015, **54**, 10225–10229.
- 10 Z. Yang, M. Zhong, X. Ma, K. Nijesh, S. De, P. Parameswaran and H. W. Roesky, *J. Am. Chem. Soc.*, 2016, **138**, 2548–2551.
- 11 W. Liu, Y. Ding, D. Jin, Q. Shen, B. Yan, X. Ma and Z. Yang, *Green Chem.*, 2019, **21**, 3812–3815.
- 12 Q. Shen, X. Ma, W. Li, W. Liu, Y. Ding, Z. Yang and H. W. Roesky, *Chem. – Eur. J.*, 2019, **25**, 11918–11923.
- 13 Y. Ding, X. Ma, Y. Liu, W. Liu, Z. Yang and H. W. Roesky, *Organometallics*, 2019, **38**, 3092–3097.
- 14 T. Chu and G. I. Nikonov, *Chem. Rev.*, 2018, **118**, 3608–3680.



- 15 V. Nesterov, D. Reiter, P. Bag, P. Frisch, R. Holzner, A. Porzelt and S. Inoue, *Chem. Rev.*, 2018, **118**, 9678–9842.
- 16 G. I. Nikonov, *ACS Catal.*, 2017, **7**, 7257–7266.
- 17 V. A. Pollard, M. Á. Fuentes, A. R. Kennedy, R. McLellan and R. E. Mulvey, *Angew. Chem., Int. Ed.*, 2018, **57**, 10651–10655.
- 18 Y. Liu, J. Li, X. Ma, Z. Yang and H. W. Roesky, *Coord. Chem. Rev.*, 2018, **374**, 387–415.
- 19 W. Li, X. Ma, M. G. Walawalkar, Z. Yang and H. W. Roesky, *Coord. Chem. Rev.*, 2017, **350**, 14–29.
- 20 L. C. Wilkins and R. L. Melen, *Coord. Chem. Rev.*, 2016, **324**, 123–139.
- 21 A. Bismuto, M. J. Cowley and S. P. Thomas, *ACS Catal.*, 2018, **8**, 2001–2005.
- 22 B. Schöffner, F. Schöffner, S. P. Verevkin and A. Börner, *Chem. Rev.*, 2010, **110**, 4554–4581.
- 23 E. Balaraman, C. Gunanathan, J. Zhang, L. J. W. Shimon and D. Milstein, *Nat. Chem.*, 2011, **3**, 609–614.
- 24 Z. Han, L. Rong, J. Wu, L. Zhang, Z. Wang and K. Ding, *Angew. Chem., Int. Ed.*, 2012, **51**, 13041–13045.
- 25 S. H. Kim and S. H. Hong, *ACS Catal.*, 2014, **4**, 3630–3636.
- 26 V. Zubar, Y. Lebedev, L. M. Azofra, L. Cavallo, O. El-Sepelgy and M. Rueping, *Angew. Chem., Int. Ed.*, 2018, **57**, 13439–13443.
- 27 A. Kumar, T. Janes, N. A. Espinosa-Jalapa and D. Milstein, *Angew. Chem., Int. Ed.*, 2018, **57**, 12076–12080.
- 28 A. Kaithal, M. Hölscher and W. Leitner, *Angew. Chem., Int. Ed.*, 2018, **57**, 13449–13453.
- 29 C. Erken, A. Kaithal, S. Sen, T. Weyhermüller, M. Hölscher, C. Werlé and W. Leitner, *Nat. Commun.*, 2018, **9**, 4521.
- 30 T. vom Stein, M. Meuresch, D. Limper, M. Schmitz, M. Hölscher, J. Coetzee, D. J. Cole-Hamilton, J. Klankermayer and W. Leitner, *J. Am. Chem. Soc.*, 2014, **136**, 13217–13225.
- 31 M. Szewczyk, M. Magre, V. Zubar and M. Rueping, *ACS Catal.*, 2019, **9**, 11634–11639.
- 32 X. Cao, W. Wang, K. Lu, W. Yao, F. Xue and M. Ma, *Dalton Trans.*, 2020, **49**, 2776–2780.
- 33 X. Xu, Z. Kang, D. Yan and M. Xue, *Chin. J. Chem.*, 2019, **37**, 1142–1146.
- 34 R. Thenarukandiyil, V. Satheesh, L. J. W. Shimon and G. Ruiter, *Chem. – Asian J.*, 2021, **16**, 999–1006.
- 35 R. F. Nystrom and W. G. Brown, *J. Am. Chem. Soc.*, 1948, **70**, 3738–3740.
- 36 M. Sutter, L. Pehlivan, R. Lafon, W. Dayoub, Y. Raoul, E. Métay and M. Lemaire, *Green Chem.*, 2013, **15**, 3020–3026.
- 37 J. Schörgenhuber, A. Zimmermann and M. Waser, *Org. Process Res. Dev.*, 2018, **22**, 862–870.
- 38 L. Le, J. Liu, T. He, D. Kim, E. J. Lindley, T. N. Cervarich, J. C. Malek, J. Pham, M. R. Buck and A. R. Chianese, *Organometallics*, 2018, **37**, 3286–3297.
- 39 D. Kim, L. Le, M. J. Drance, K. H. Jensen, K. Bogdanovski, T. N. Cervarich, M. G. Barnard, N. J. Pudalov, S. M. M. Knapp and A. R. Chianese, *Organometallics*, 2016, **35**, 982–989.
- 40 K. Junge, B. Wendt, A. Cingolani, A. Spannenberg, Z. Wei, H. Jiao and M. Beller, *Chem. – Eur. J.*, 2018, **24**, 1046–1052.
- 41 T. J. Korstanje, J. I. v. d. Vlugt, C. J. Elsevier and B. D. Bruin, *Science*, 2015, **350**, 298–302.
- 42 J. Yuwen, S. Chakraborty, W. W. Brennessel and W. D. Jones, *ACS Catal.*, 2017, **7**, 3735–3740.
- 43 M. Arrowsmith, M. S. Hill, T. Hadlington, G. Kociok-Köhn and C. Weetman, *Organometallics*, 2011, **30**, 5556–5559.
- 44 D. Mukherjee, A. Ellern and A. D. Sadow, *Chem. Sci.*, 2014, **5**, 959–964.
- 45 D. Mukherjee, S. Shirase, T. P. Spaniol, K. Mashima and J. Okuda, *Chem. Commun.*, 2016, **52**, 13155–13158.
- 46 M. K. Barman, A. Baishya and S. Nembenna, *Dalton Trans.*, 2017, **46**, 4152–4156.
- 47 C. J. Barger, A. Motta, V. L. Weidner, T. L. Lohr and T. J. Marks, *ACS Catal.*, 2019, **9**, 9015–9024.
- 48 A. Y. Khalimon, P. Farha, L. G. Kuzmina and G. I. Nikonov, *Chem. Commun.*, 2012, **48**, 455–457.
- 49 C. C. Chong and R. Kinjo, *ACS Catal.*, 2015, **5**, 3238–3259.
- 50 J. Magano and J. R. Dunetz, *Org. Process Res. Dev.*, 2012, **16**, 1156–1184.
- 51 B. T. Cho, *Chem. Soc. Rev.*, 2009, **38**, 443–452.
- 52 S. Chakraborty, P. Bhattacharya, H. Dai and H. Guan, *Acc. Chem. Res.*, 2015, **48**, 1995–2003.
- 53 J. V. B. Kanth and M. Periasamy, *J. Org. Chem.*, 1991, **56**, 5964–5965.
- 54 Y. Suseela and M. Periasamy, *Tetrahedron*, 1992, **48**, 371–376.
- 55 X. Cui, Y. Li, C. Topf, K. Junge and M. Beller, *Angew. Chem., Int. Ed.*, 2015, **54**, 10596–10599.
- 56 T. P. Brewster, A. J. M. Miller, D. M. Heinekey and K. I. Goldberg, *J. Am. Chem. Soc.*, 2013, **135**, 16022–16025.
- 57 M. Zhang, N. Li, X. Tao, R. Ruzi, S. Yu and C. Zhu, *Chem. Commun.*, 2017, **53**, 10228–10231.
- 58 Y. Corre, V. Rysak, X. Trivelli, F. Agbossou-Niedercorn and C. Michon, *Eur. J. Org. Chem.*, 2017, 4820–4826.
- 59 T. V. Q. Nguyen, W. J. Yoo and S. Kobayashi, *Adv. Synth. Catal.*, 2016, **358**, 452–458.
- 60 J. A. Fernández-Salas, S. Manzini and S. P. Nolan, *Adv. Synth. Catal.*, 2014, **356**, 308–312.
- 61 J. Zheng, S. Chevance, C. Darcel and J.-B. Sortais, *Chem. Commun.*, 2013, **49**, 10010–10012.
- 62 L. C. Misal Castro, H. Li, J.-B. Sortais and C. Darcel, *Chem. Commun.*, 2012, **48**, 10514–10516.
- 63 K. Matsubara, T. Iura, T. Maki and H. Nagashima, *J. Org. Chem.*, 2002, **67**, 4985–4988.
- 64 V. Gevorgyan, M. Rubin, J.-X. Liu and Y. Yamamoto, *J. Org. Chem.*, 2001, **66**, 1672–1675.
- 65 S. Kisan, V. Krishnakumar and C. Gunanathan, *ACS Catal.*, 2018, **8**, 4772–4776.
- 66 M. K. Barman, K. Das and B. Maji, *J. Org. Chem.*, 2019, **84**, 1570–1579.



- 67 Y. Zheng, X. Cao, J. Li, H. Hua, W. Yao, B. Zhao and M. Ma, *Chin. J. Org. Chem.*, 2020, **40**, 2086–2093.
- 68 A. Harinath, J. Bhattacharjee and T. K. Panda, *Chem. Commun.*, 2019, **55**, 1386–1389.
- 69 W. Wang, M. Luo, D. Zhu, W. Yao, L. Xu and M. Ma, *Org. Biomol. Chem.*, 2019, **17**, 3604–3608.
- 70 X. Xu, D. Yan, Z. Zhu, Z. Kang, Y. Yao, Q. Shen and M. Xue, *ACS Omega*, 2019, **4**, 6775–6783.
- 71 T. Sakakura, J.-C. Choi and H. Yasuda, *Chem. Rev.*, 2007, **107**, 2365–2387.
- 72 M. Cokoja, C. Bruckmeier, B. Rieger, W. A. Herrmann and F. E. Kühn, *Angew. Chem., Int. Ed.*, 2011, **50**, 8510–8537.
- 73 M. Peters, B. Köhler, W. Kuckshinrichs, W. Leitner, P. Markewitz and T. E. Müller, *ChemSusChem*, 2011, **4**, 1216–1240.
- 74 A. Goeppert, M. Czaun, J.-P. Jones, G. K. Surya Prakash and G. A. Olah, *Chem. Soc. Rev.*, 2014, **43**, 7995–8048.
- 75 Q. Liu, L. Wu, R. Jackstell and M. Beller, *Nat. Commun.*, 2015, **6**, 5933.
- 76 J. Klankermayer, S. Wesselbaum, K. Beydoun and W. Leitner, *Angew. Chem., Int. Ed.*, 2016, **55**, 7296–7343.
- 77 J. Artz, T. E. Müller, K. Thenert, J. Kleinekorte, R. Meys, A. Sternberg, A. Bardow and W. Leitner, *Chem. Rev.*, 2017, **118**, 434–504.
- 78 W.-H. Wang, Y. Himeda, J. T. Muckerman, G. F. Manbeck and E. Fujita, *Chem. Rev.*, 2015, **115**, 12936–12973.
- 79 W. H. Bernskoetter and N. Hazari, *Acc. Chem. Res.*, 2017, **50**, 1049–1058.
- 80 K. Sordakis, C. Tang, L. K. Vogt, H. Junge, P. J. Dyson, M. Beller and G. Laurenczy, *Chem. Rev.*, 2017, **118**, 372–433.
- 81 S. Chakraborty, J. Zhang, J. A. Krause and H. Guan, *J. Am. Chem. Soc.*, 2010, **132**, 8872–8873.
- 82 L. J. Murphy, H. Hollenhorst, R. McDonald, M. Ferguson, M. D. Lumsden and L. Turculet, *Organometallics*, 2017, **36**, 3709–3720.
- 83 H.-W. Suh, L. M. Guard and N. Hazari, *Chem. Sci.*, 2014, **5**, 3859–3872.
- 84 S. Bontemps, L. Vendier and S. Sabo-Etienne, *J. Am. Chem. Soc.*, 2014, **136**, 4419–4425.
- 85 M. R. Espinosa, D. J. Charboneau, A. Garcia de Oliveira and N. Hazari, *ACS Catal.*, 2018, **9**, 301–314.
- 86 R. Shintani and K. Nozaki, *Organometallics*, 2013, **32**, 2459–2462.
- 87 G. Jin, C. G. Werncke, Y. Escudié, S. Sabo-Etienne and S. Bontemps, *J. Am. Chem. Soc.*, 2015, **137**, 9563–9566.
- 88 S. Bontemps, L. Vendier and S. Sabo-Etienne, *Angew. Chem., Int. Ed.*, 2012, **51**, 1671–1674.
- 89 T. Janes, K. M. Osten, A. Pantaleo, E. Yan, Y. Yang and D. Song, *Chem. Commun.*, 2016, **52**, 4148–4151.
- 90 S. R. Tamang and M. Findlater, *Dalton Trans.*, 2018, **47**, 8199–8203.
- 91 X. Wang, K. Chang and X. Xu, *Dalton Trans.*, 2020, **49**, 7324–7327.
- 92 D. Mukherjee, H. Osseili, T. P. Spaniol and J. Okuda, *J. Am. Chem. Soc.*, 2016, **138**, 10790–10793.
- 93 M.-A. Courtemanche, M.-A. Légaré, L. Maron and F.-G. Fontaine, *J. Am. Chem. Soc.*, 2013, **135**, 9326–9329.
- 94 M.-A. Courtemanche, M.-A. Légaré, L. Maron and F.-G. Fontaine, *J. Am. Chem. Soc.*, 2014, **136**, 10708–10717.
- 95 T. Wang and D. W. Stephan, *Chem. – Eur. J.*, 2014, **20**, 3036–3039.
- 96 N. von Wolff, G. Lefèvre, J. C. Berthet, P. Thuéry and T. Cantat, *ACS Catal.*, 2016, **6**, 4526–4535.
- 97 A. D. Bage, T. A. Hunt and S. P. Thomas, *Org. Lett.*, 2020, **22**, 4107–4112.
- 98 D. Franz, C. Jandl, C. Stark and S. Inoue, *ChemCatChem*, 2019, **11**, 5275–5281.
- 99 M.-A. Courtemanche, J. Larouche, M.-A. Légaré, W. Bi, L. Maron and F.-G. Fontaine, *Organometallics*, 2013, **32**, 6804–6811.
- 100 C.-C. Chia, Y.-C. Teo, N. Cham, S. Y.-F. Ho, Z.-H. Ng, H.-M. Toh, N. Mézailles and C.-W. So, *Inorg. Chem.*, 2021, **60**, 4569–4577.
- 101 A. Caise, D. Jones, E. L. Kolychev, J. Hicks, J. M. Goicoechea and S. Aldridge, *Chem. – Eur. J.*, 2018, **24**, 13624–13635.
- 102 D. Sarkar, C. Weetman, S. Dutta, E. Schubert, C. Jandl, D. Koley and S. Inoue, *J. Am. Chem. Soc.*, 2020, **142**, 15403–15411.
- 103 D. Sarkar, S. Dutta, C. Weetman, E. Schubert, D. Koley and S. Inoue, *Chem. – Eur. J.*, 2021, **27**, 13072–13078.
- 104 K. Kitaura and K. Morokuma, *Int. J. Quantum Chem.*, 1976, **10**, 325–340.
- 105 F. M. Bickelhaupt and K. N. Houk, *Angew. Chem., Int. Ed.*, 2017, **56**, 10070–10086.
- 106 S. Dutta, K. Singh and D. Koley, *Chem. – Asian J.*, 2021, **16**, 3492–3508.

